



ELSEVIER

Contents lists available at ScienceDirect

EBioMedicine

journal homepage: www.elsevier.com/locate/ebiom

Research paper

Biallelic mutations in LAMA5 disrupts a skeletal noncanonical focal adhesion pathway and produces a distinct bent bone dysplasia

Maya Barad^a, Fabiana Csukasi^{a,b}, Michaela Bosakova^{c,d}, Jorge H. Martin^a, Wenjuan Zhang^e, S. Paige Taylor^a, Ralph S. Lachman^f, Jennifer Zieba^a, Michael Bamshad^g, Deborah Nickerson^g, Jessica X. Chong^g, Daniel H. Cohn^{a,e,h}, Pavel Krejci^{c,d}, Deborah Krakow^{a,f,h,i,j,#,*}, Ivan Duran^{a,b,k,#}

^a Department of Orthopaedic Surgery, University of California—Los Angeles, 615 Charles E. Young Drive South, BSRB 512, Los Angeles, CA 90095, United States

^b Laboratory of Bioengineering and Tissue Regeneration-LABRET, Department of Cell Biology, Genetics and Physiology, University of Málaga, IBIMA, Málaga 29071, Spain

^c Department of Biology, Faculty of Medicine, Masaryk University, Brno 62500, Czech Republic

^d International Clinical Research Center, St. Anne's University Hospital, Brno 65691, Czech Republic

^e Department of Molecular, Cell and Developmental Biology, University of California—Los Angeles, Los Angeles, CA 90095, United States

^f International Skeletal Dysplasia Registry, University of California, Los Angeles, CA 90095 United States

^g University of Washington Center for Mendelian Genomics, University of Washington, Seattle, WA 98195 United States

^h Orthopaedic Institute for Children, University of California—Los Angeles, Los Angeles, CA 90095, United States

ⁱ Department of Human Genetics, University of California—Los Angeles, Los Angeles, CA 90095, United States

^j Department of Obstetrics and Gynecology, University of California—Los Angeles, Los Angeles, CA 90095, United States

^k Networking Biomedical Research Center in Bioengineering, Biomaterials and Nanomedicine (CIBER-BBN), Andalusian Centre for Nanomedicine and Biotechnology-BIONAND, Severo Ochoa 35, Málaga 29590, Spain



ARTICLE INFO

Article History:

Received 28 July 2020

Revised 30 September 2020

Accepted 1 October 2020

Available online xxx

Keywords:

Laminin $\alpha 5$

LAMA5

Skeletal dysplasia

Bent bone

$\beta 1$ integrin

ABSTRACT

Background: Beyond its structural role in the skeleton, the extracellular matrix (ECM), particularly basement membrane proteins, facilitates communication with intracellular signaling pathways and cell to cell interactions to control differentiation, proliferation, migration and survival. Alterations in extracellular proteins cause a number of skeletal disorders, yet the consequences of an abnormal ECM on cellular communication remains less well understood

Methods: Clinical and radiographic examinations defined the phenotype in this unappreciated bent bone skeletal disorder. Exome analysis identified the genetic alteration, confirmed by Sanger sequencing. Quantitative PCR, western blot analyses, immunohistochemistry, luciferase assay for WNT signaling were employed to determine RNA, proteins levels and localization, and dissect out the underlying cell signaling abnormalities. Migration and wound healing assays examined cell migration properties.

Findings: This bent bone dysplasia resulted from biallelic mutations in *LAMA5*, the gene encoding the alpha-5 laminin basement membrane protein. This finding uncovered a mechanism of disease driven by ECM-cell interactions between alpha-5-containing laminins, and integrin-mediated focal adhesion signaling, particularly in cartilage. Loss of *LAMA5* altered $\beta 1$ integrin signaling through the non-canonical kinase PYK2 and the skeletal enriched SRC kinase, FYN. Loss of *LAMA5* negatively impacted the actin cytoskeleton, vinculin localization, and WNT signaling.

Interpretation: This newly described mechanism revealed a *LAMA5*- $\beta 1$ Integrin-PYK2-FYN focal adhesion complex that regulates skeletogenesis, impacted WNT signaling and, when dysregulated, produced a distinct skeletal disorder.

Funding: Supported by NIH awards R01 AR066124, R01 DE019567, R01 HD070394, and U54HG006493, and Czech Republic grants INTER-ACTION LTAUSA19030, V18-08-00567 and GA19-20123S.

© 2020 The Authors. Published by Elsevier B.V. This is an open access article under the CC BY-NC-ND license (<http://creativecommons.org/licenses/by-nc-nd/4.0/>)

1. Introduction

For proper intracellular function, cells need to interact with their extracellular matrix (ECM). The ECM provides a structural scaffold for the cell and aids in the maintenance of contacts between neighboring

* Corresponding author.

E-mail address: dkrakow@mednet.ucla.edu (D. Krakow).

Co-senior authors

Research in context

Evidence before this study

Prior to this work, there remains heritable disorders of the bone and cartilage, the osteochondrodysplasias, for which the molecular basis is unknown. This includes a group of disorders that are referred to as bent bone dysplasias in the recent nosology of the osteochondrodysplasias. Not all clinical and radiographic phenotypes fit into the well classified disorders for which the molecular basis has been established and there remain affected individuals with no basis for their disease.

Added value of this study

This study uncovers a newly described skeletal disorder associated with multiple skeletal defects including distinct bending of long bones, contractures, dysmorphic facies and lethality. Using exome analysis, biallelic mutations in the gene encoding *LAMA5* co-segregated with the disorder. These mutations led to diminished *LAMA5* expression including in cartilage. Immunohistochemistry showed that *LAMA5* is well expressed in musculoskeletal tissues. Loss of *LAMA5* led to decreased $\beta 1$ integrin signaling through a noncanonical pathway that affected focal adhesion complexes, uncovering a network, *LAMA5*- $\beta 1$ Integrin-PYK2-FYN. Further, diminished *LAMA5* negatively impacted the actin cytoskeleton, vinculin localization, and WNT signaling, tying focal adhesion molecules to key skeletal signaling molecules.

Implications of all available evidence

This work uncovered a role for *LAMA5* in regulating skeletogenesis and that *LAMA5* mutations can produce a recessively inherited skeletal dysplasia. In chondrocytes, *LAMA5* regulated $\beta 1$ Integrin signaling in a cell context manner. This work further demonstrates the importance of basement membrane proteins and the role of $\beta 1$ integrin signaling in the skeleton.

induces clustering and maturation of these integrin focal points [11]. This clustering promotes the growth of focal adhesions through phosphorylation of other focal adhesion kinases with subsequent activation of the SRC family kinases and p130CAS [12]. These focal adhesion kinases compose the integrin adhesome and are crucial in determining downstream signaling events, culminating in changes in cell fate and behavior.

Skeletal dysplasias include over 460 defined heritable disorders of bone and cartilage diagnosed through a combination of clinical, radiographic and molecular findings [13]. Bending of bones is a phenotypic finding in many of the well-defined skeletal disorders including campomelic dysplasia [14], osteogenesis imperfecta [15], hypophosphatasia, and bent bone dysplasia FGFR2 type [16], among others [17, 18]. Underlying genetic causes in these disorders are distinct and include mutations in genes that encode transcription factors, collagens, enzymes, and receptors. Herein, we delineate a previously undescribed bent bone skeletal dysplasia resulting from biallelic mutations in *LAMA5*, which encodes the $\alpha 5$ laminin subunit (*LAMA5*). The mutations resulted in reduced *LAMA5* expression and alterations in the integrin focal adhesion pathway involving the non-canonical downstream kinases, PYK2 and FYN. Loss of *LAMA5* also altered proper localization of cellular vinculin and diminished WNT signaling. These findings support the importance of proper focal adhesion induced signaling through *LAMA5*-Integrin $\beta 1$ -PYK2-FYN signaling in skeletal development and identify a novel skeletal disorder resulting from disruption of the signaling pathway.

2. Results

2.1. Mutations in *LAMA5* result in a new form of bent bone dysplasia

We identified three siblings from a single nonconsanguineous family (International Skeletal Dysplasia Registry reference number R03–206) with skeletal defects that did not phenotypically or radiographically match any of the currently classified skeletal disorders. Clinical findings included atrial septal defects, relative macrocephaly, micrognathia, proptosis, ear abnormalities, widely spaced nipples, elbow dislocations, and severe distal limb contractures (Table S1). Additionally, there was significant polyhydramnios in the prenatal period suggesting placental dysfunction or fetal inability to swallow properly. Radiographic findings included under-mineralization of the calvarium (Fig. 1a-b and S1), distinctly bent, under-mineralized long bones, particularly of the femora, with mid-diaphyseal angulation (Fig. 1c-e and S1), platyspondyly with coronal clefts (Fig. 1f-g and S1), hypoplastic acetabular roofs with femoral head dislocation, (Fig. 1e and S1), and bilateral upper and lower extremity contractures (Fig. 1h-j and S1). The three affected individuals all delivered at term but died shortly after birth due to presumed pulmonary insufficiency, even though their chests were not small. Detailed phenotypic, radiographic and histologic findings for each affected individual are described in Supplementary Table 1. The clinical and radiographic findings suggested an unclassified or previously undescribed skeletal disorder.

Exome sequence analyses on the 3 affected individuals, one unaffected sibling, and the parents (Fig. 2a) demonstrated that the affected individuals had biallelic mutations in *LAMA5* [OMIM 601,033]. The affected siblings and the father (R03–206-E, -A, -B, -G) (Fig. 2b) were heterozygous for the missense variant, NG_050626.1:g.43161G>A (c.4213G>A), predicted to result in the amino acid substitution p.Ala1405Thr, corresponding to a region close to the central cluster of epidermal growth factor (EGF) domains within the protein (Fig. 2c). The g.43161G>A variant has an allele frequency of 0.0006 in the gnomAD database (<https://gnomad.broadinstitute.org/>) and has not been seen in the homozygous state. Further this alanine at position 1405 is either an alanine or glycine, among all vertebrates, and threonine is not one seen at position p.1405 in any species. Using the

cells. Dependent on the tissue type, cells produce an ECM that is primarily composed of two classes of macromolecules, fibrous proteins and proteoglycans. ECM fibrous proteins include collagens, fibronectins, elastins, and laminins [1]. While collagens are the most abundant fibrous ECM proteins [1], laminins are the major components of the basement membrane, a specialized ECM immediately surrounding the cell [2, 3]. Laminins are composed of α , β and γ polypeptide chains that self-assemble through their coiled coil domains into a T-shape configuration achieved by disulfide bonds along their long arms [4]. To date, five α , four β and three γ chains have been identified, and 16 distinct combinations of these chains have been delineated [4, 5]. Basement membranes provide cells with physical scaffolding and tensile strength and, through binding partners, participate in cellular differentiation and homeostasis.

In addition to supplying physical support to cells, the ECM participates in biologic functions due to its ability to bind multiple interacting partners that include growth factors, signal receptors, and adhesion molecules [6]. Adhesion molecules are cell surface glycoproteins involved in cell-to-cell and cell-to-ECM interactions and include the following protein families: integrins, the immunoglobulin superfamily, selectins, and cadherins [7]. Among the adhesion molecules, integrins interact with ECM collagens, fibronectin, and laminins to generate a multi-protein focal adhesion complex required for communication between the ECM and the actin cytoskeleton [8–10]. Upon integrin signaling, talin and paxillin recruit the focal adhesion kinases (FAK or PYK2) and then the cytoskeletal protein vinculin

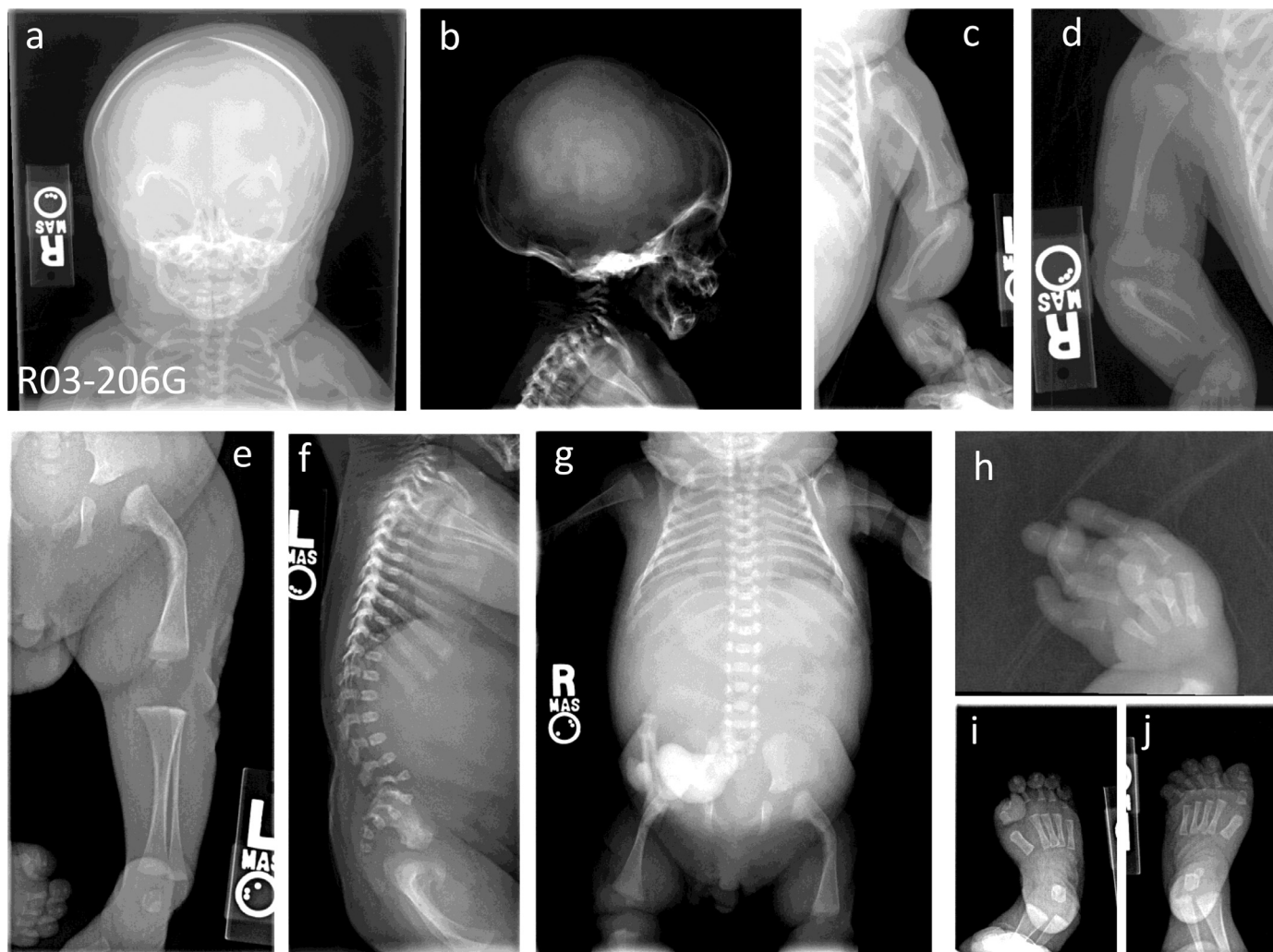


Fig. 1. Radiographic findings in R03–206 G. Full term fetus with enlarged skull (a), micrognathia (b), presence of scapula and elbow dislocations (c), slight bowing of the humerus, radius and ulna (c, d), severely bent femurs with cortical abnormalities (e), platyspondyly with coronal clefts (f), aplastic acetabular roofs (g) ulnar deviation and contractures in the hands (h) and bilateral equinovarus (i, j).

Mutationtaster prediction program (<http://www.mutationtaster.org>), the variant is presumed to be “disease causing” with a score of 0.57 by Bayes classifier, though it was classified as benign by SIFT (<http://sift.jcvi.org>). The second variant, NG_050626.1:g.49646C>T (c.6157C>T), was present in all affected siblings and the mother (R03-206-D, -A, -B, -G) (Fig. 2b) and it is predicted to result in the amino acid substitution, p.Arg2053Cys, affecting one of the central EGF-like domains (Fig. 2c). This variant, g.49655C>T has an allele frequency of 0.0003, also has not been reported in the homozygous state, and is classified as “disease causing” with a score of 0.99 by Bayes classifier (Mutationtaster prediction algorithm), though also classified as benign by the SIFT program. This residue is conserved as an arginine to *c.elegans*, though it is a similarly positively charged histidine in *r.norvegicus* and *g.gallus*. One unaffected sibling R03-206H, was a carrier of the c.4213G>A variant, predicting the p. Ala1405Thr substitution. Because all three affected siblings were compound heterozygotes for both mutations and each parent carried of one of the variants, the inheritance pattern was consistent with an autosomal recessive disorder. Both mutations affected the protein in or near EGF-like domains involved in disulfide bonding, which are essential for proper folding and secretion of the mature protein (Fig. 2c).

At the protein level, studies using primary chondrocytes, fibroblasts and cartilage derived from one of the affected individuals (R03-206G), showed statistically significantly decreased levels of

LAMA5, demonstrating that the mutations in *LAMA5* destabilized the protein (Fig. 2d-f), supporting the conclusion that decreased LAMA5 produced this unclassified bent bone dysplasia.

2.2. *LAMA5* expression in the musculoskeletal tissues and colocalization with focal adhesion components around skeletal blood vessels

The role of LAMA5 in the skeleton has not been well investigated. However, recent evidence suggests that laminins containing the alpha5 subunit participate in bone homeostasis through cell to matrix interactions, particularly around type E blood vessels [19]. To obtain a deeper understanding of the role played by LAMA5 in the skeleton, we first used publicly available data to examine gene expression in bone and cartilage tissues; *LAMA5* showed broad expression that included cartilage and bone (Figure S2a) [20, 21]. We then used immunostaining of several human musculoskeletal tissues with LAMA5 antibodies and demonstrated expression of the protein around blood vessels in cartilage and ligament (Fig. 3a, c-d), as well as in muscle, ligaments, periosteum, trabecular bone and throughout the cartilage, particularly in the growth plate and in articular chondrocytes (Fig. 3a-g). LAMA5 was similarly distributed in mouse musculoskeletal tissues (Figure S2B). CD34, a marker for the specialized capillary subtype E that is strongly linked to osteogenesis through $\beta 1$ integrin and LAMA5 interactions [19] showed a similar localization to LAMA5 in the vascular system of cartilage and in ligaments and bone

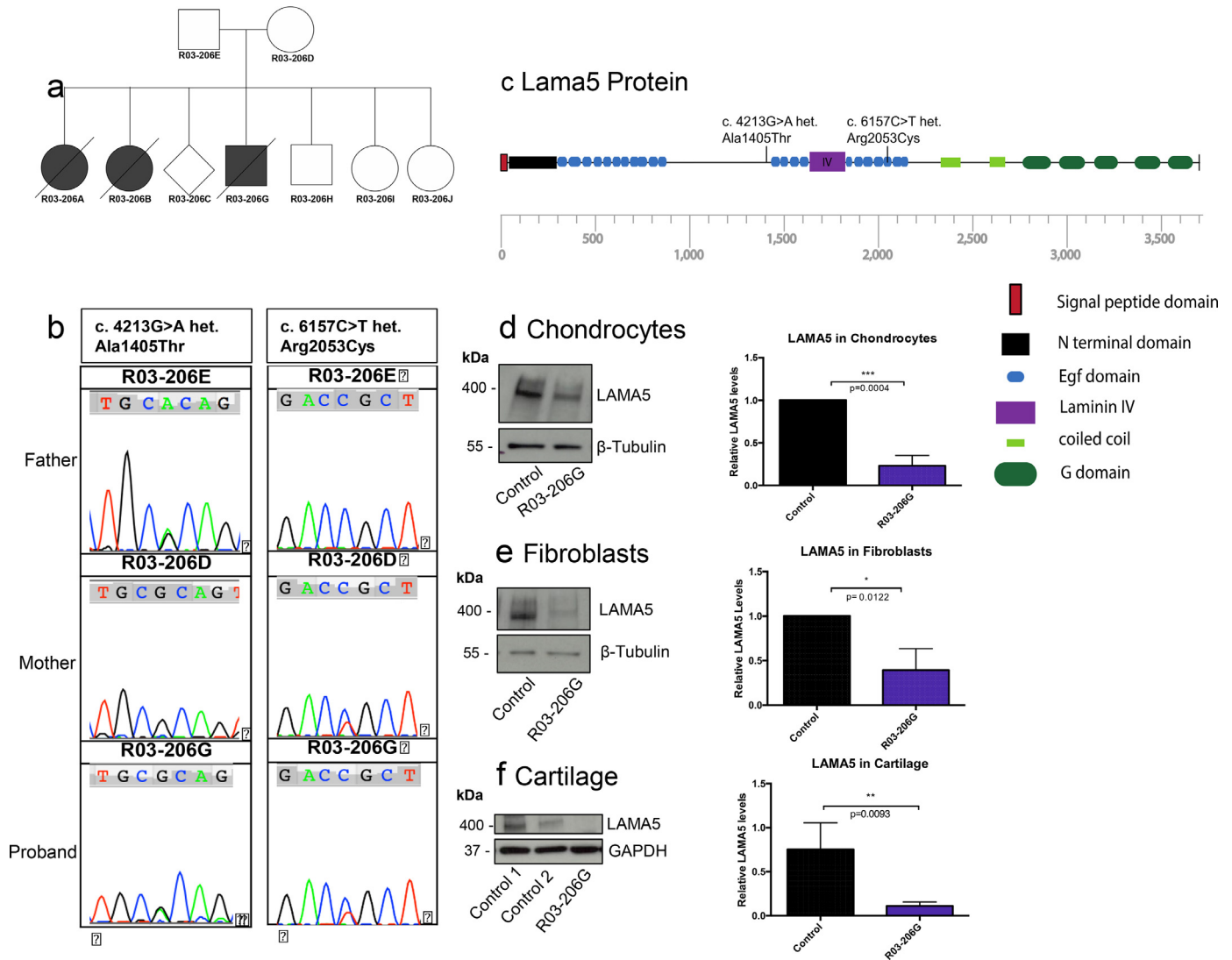


Fig. 2. Compound heterozygous missense mutations in *LAMA5* destabilize the $\alpha 5$ laminin subunit. (a) Three affected siblings (R03–206A, B, C) showed the bent bone dysplasia phenotype. (b) Each parent (R03–206E, D) carried one of the mutations. (c) The mutations localized close to EGF domains of the *LAMA5* protein. (d, e) Affected patient derived chondrocytes and fibroblasts showed reduced levels of *LAMA5*, * $p < 0.05$, ** $p < 0.01$. (f) Similar reduction was observed in cartilage derived from the affected individual R03–206 G, *** $p < 0.001$.

(Fig S2C). Because of the established role of *LAMA5* in integrin signaling and focal adhesions, p130-CAS (Figure S2d), a downstream component of the integrin adhesion intracellular cascade was also interrogated and, similar to *LAMA5*, was expressed in blood vessels, articular cartilage, ligament, and trabecular bone. These results showed that there is a broad distribution of *LAMA5* in musculoskeletal tissues, including tissue blood vessels, and that *LAMA5* co-localized with p130-CAS, a component of the integrin-focal adhesion pathway.

2.3. *LAMA5* mutations alter a non-canonical focal adhesion signaling pathway

Laminins interact with integrins on the cell surfaces of multiple cell lineages. More specifically, *LAMA5* laminins have been shown to interact with integrin receptors containing the $\beta 1$ subunit in specialized bone endothelial lineages supporting osteogenesis [19]. To further study the connection between *LAMA5* and integrin signaling in the skeleton, we analyzed different components of the integrin-focal adhesion pathway in primary chondrocytes derived from control and affected individuals and in a gene-edited HeLa cell line, a cell line with a high expression of *LAMA5*. The HeLa cell mutation is a single

nucleotide insertion (317insA) and results in alternative splicing in exon 2, deleting 51 amino acids in the short arm of *LAMA5* (Canopy Biosciences, KOCE0011980). The mutation is a hypomorphic allele (*LAMA5*^{Hyp}) which in the homozygous state reduced *LAMA5* protein by 88% (Fig. 4B–D), similar to the levels found in the patient-derived tissues with biallelic *LAMA5* mutations. In the R03–208G chondrocytes, the level of $\beta 1$ integrin was decreased (Fig. 4a, e), suggesting the potential for a lack of proper integrin signaling. In the *LAMA5*^{Hyp/Hyp} cells, not only was there decreased mature $\beta 1$ -integrin (Fig. 4b, f), but also a pattern consistent with accumulation of immature forms of the protein in the secretory pathway [22]. Activation of the integrin receptors by laminins usually initiates the formation of the focal adhesion complex by phosphorylation of Focal Adhesion Kinase (FAK), the main intracellular integrin signal transducer. FAK subsequently triggers phosphorylation of the SRC family kinases p130CAS and Paxillin in order to reorganize the actin cytoskeleton and decrease integrin turnover [23, 24]. Although protein levels of the $\beta 1$ -integrin receptors were altered in defective *LAMA5* cells, levels of phosphorylated FAK were not altered in either patient chondrocytes or *LAMA5*^{Hyp/Hyp} cells (Fig. 4a–b and S3a–b).

As canonical integrin signaling through FAK was not affected, we interrogated alternative components of the focal adhesion pathway.

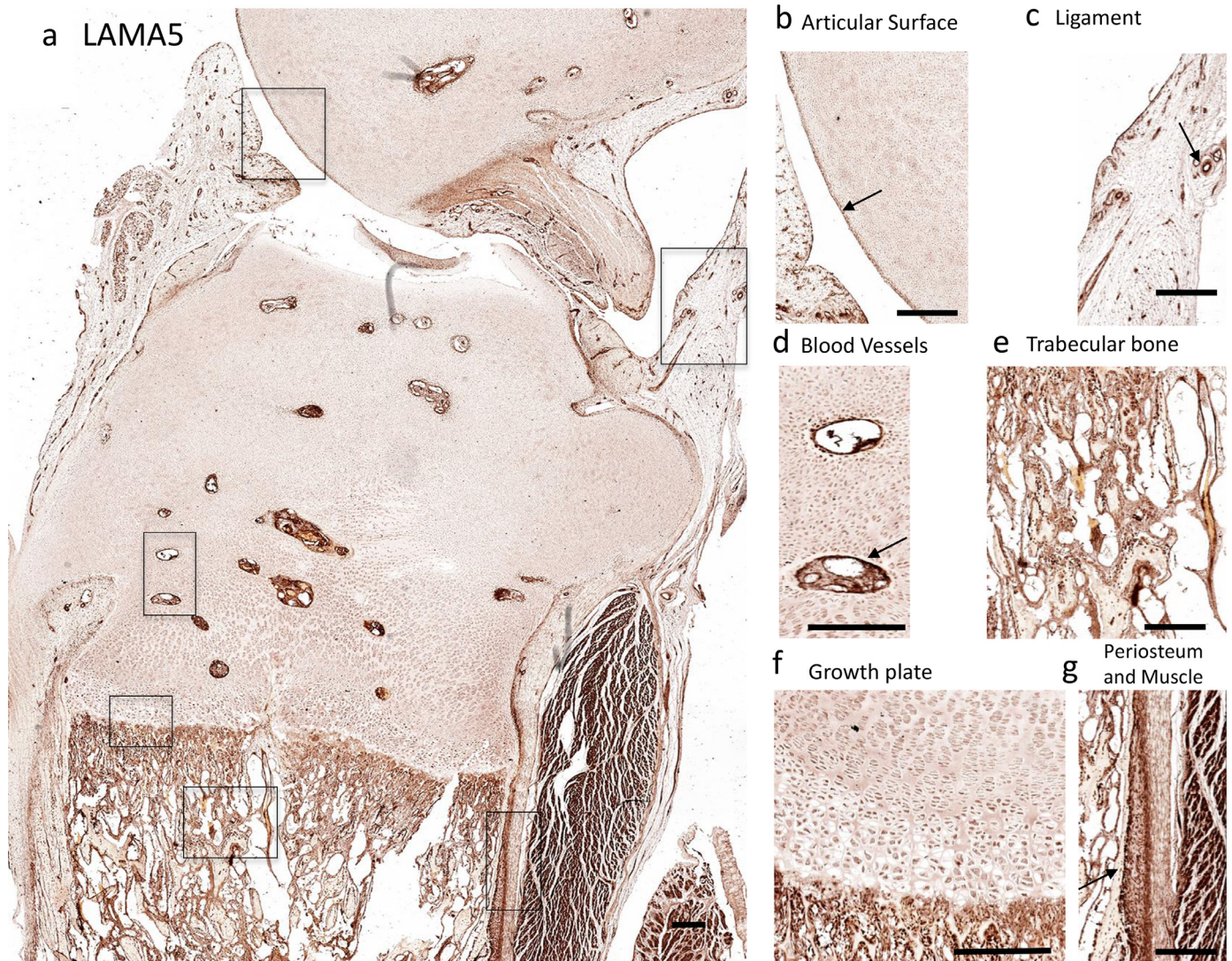


Fig. 3. LAMA5 localization in the skeleton. (a) LAMA5 staining in a fetal 18 week musculoskeletal tissues. LAMA5 localized around blood vessels in cartilage, ligaments and bone (c-e) and independently of blood vessels in articular cartilage, periosteum and growth plate (b, g, f). Bars represent 50 μm .

Proline-rich tyrosine kinase 2 (PYK2) is a non-receptor tyrosine kinase member of the FAK family with a similar role, but its expression pattern is restricted to only a few tissues, among them bone and cartilage [25–27]. Like FAK, PYK2 is also established as a scaffold for the SRC family of kinases and its translocation to focal adhesions promotes its association with the focal adhesion proteins p130-CAS and Paxillin. Relative to controls, both phosphorylated and total PYK2 levels were decreased in bent bone *LAMA5* and HeLa *LAMA5*^{Hyp/Hyp} mutant cells (Fig. 4a–b and g–j). Further studies of the integrin focal adhesion complex also showed decreased levels in general downstream phosphorylation of p-P130Cas and p-Paxillin (Fig. 4a–b and k–n).

2.4. Noncanonical PYK2 and SRC family member FYN expression in musculoskeletal tissues

Since PYK2 expression was diminished, as well as the total phosphorylated SRC family (Fig. 5a–b and S3e–f), we sought to understand which SRC family kinase member(s) were highly expressed in bone and cartilage, two of the main tissues involved in this skeletal disorder. Publicly available transcriptional data for SRC family members FGR, FYN, YES1, LYN1, BLK, cSRC, LCK, HCK,

and FRK, showed high levels of FYN expression in both cartilage and bone [21, 28]. Thus, we interrogated the *LAMA5*^{Hyp/Hyp} HeLa cells, demonstrating that FYN levels were decreased compared to control (Fig. 5b–c). The data suggested that decreased FYN levels, correlated with decreased phosphorylation levels of general SRC resulted from changes in integrin signaling caused by deficient levels of LAMA5.

As both PYK2 and FYN levels were decreased in *LAMA5*^{Hyp/Hyp} cells, we investigated their skeletal tissue localization relative to LAMA5 by immunohistochemistry. Very similar to LAMA5, PYK2 was localized in cartilage around blood vessels, in the articular cartilage, the cartilage growth plate, periosteum/perichondrium, ligaments and trabecular bone (Fig. 5d–j). Furthermore, FYN expression was comparable to PYK2 and LAMA5, with expression in articular cartilage, cartilage blood vessels, ligaments, perichondrium, and primary spongiosum, but with no expression in the proliferative and hypertrophic zones of the cartilage growth plate. (Fig. 5k–q). These findings show that key downstream signaling components in the $\beta 1$ integrin cascade altered by loss of LAMA5 signaling, PYK2 and FYN, share overlapping expression in skeletal tissues, supporting a mechanism involving these molecules in producing this skeletal dysplasia.

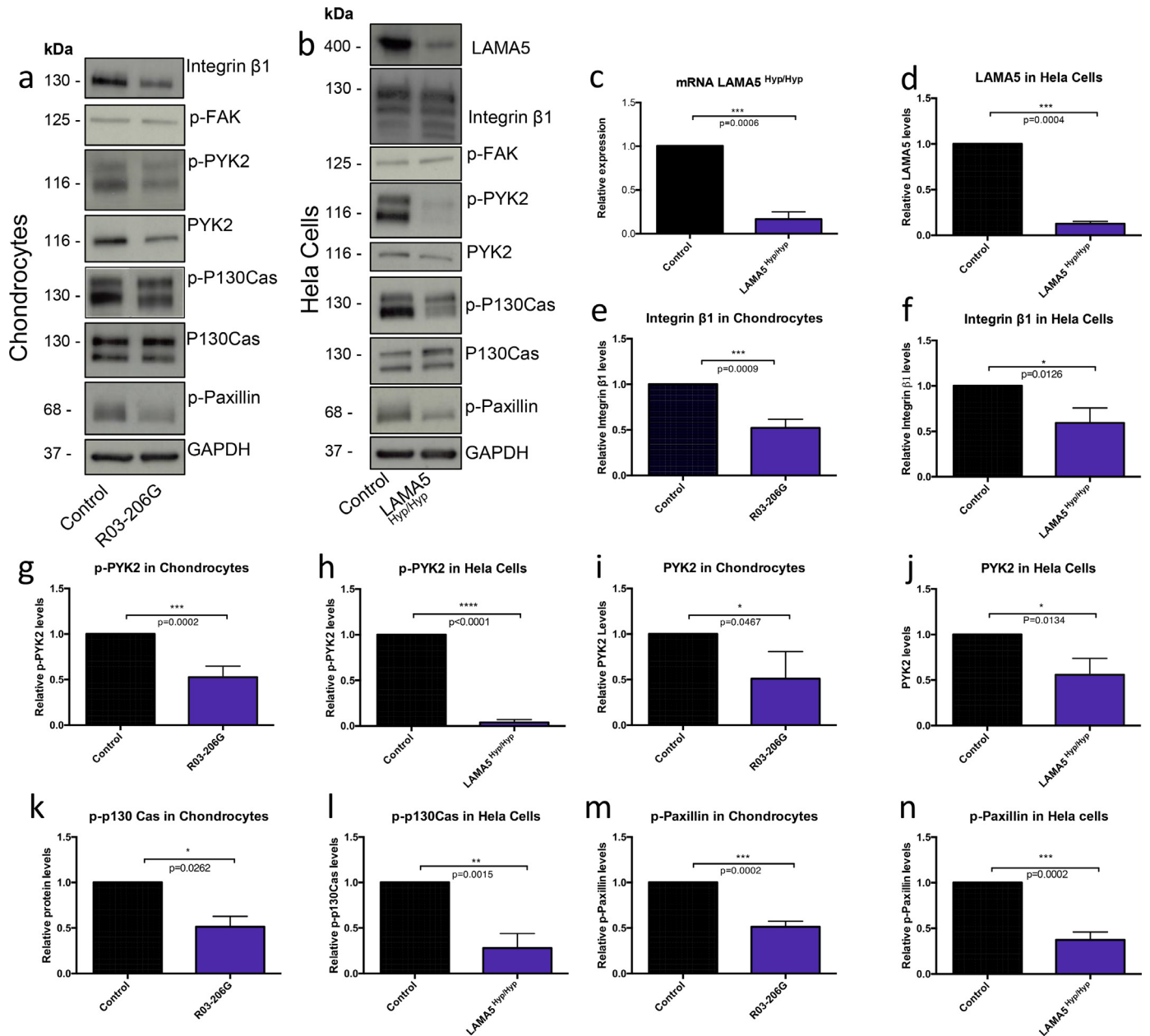


Fig. 4. Deficient LAMA5 disrupts the focal adhesion pathway. (a) Chondrocytes from R03–206G showed decreased levels of integrin $\beta 1$, total PYK2, pPYK2, p-P130CAS, and pPaxillin. (b) Similar changes were observed in HeLa LAMA5^{Hyp/Hyp}. (c) Quantitative PCR statistical analysis of the expression of gene-edited HeLa cells with the LAMA5^{Hyp/Hyp} allele. (d–n) Quantification of protein levels in chondrocytes and HeLa cells from a and b, * $p < 0.05$, ** $p < 0.01$, *** $p < 0.001$, **** $p < 0.0001$.

2.5. Effects on cell adhesion due to loss of LAMA5

Laminin-integrin interactions activate the focal adhesion pathway, bringing vinculin (VCL) to the complex in order to connect the extracellular matrix to the actin cytoskeleton [29]. While loss of LAMA5 decreased expression of the $\beta 1$ integrin focal adhesion proteins, no changes were detected in the total protein levels of VCL in LAMA5 mutant chondrocytes or LAMA5^{Hyp/Hyp} HeLa cells (Fig 6a–d). Since the total amount of intracellular VCL was unaltered, we examined whether mutant LAMA5 dysregulated focal adhesion formation through VCL mislocalization by visualizing focal adhesions in LAMA5^{Hyp/Hyp} cell cultures. Actin staining showed a disorganized cytoskeleton and there was a reduced number of VCL focal adhesions in LAMA5^{Hyp/Hyp} cells (Fig. 6e–f). This reduction in focal adhesions was confirmed using functional assays of cell adhesion and proliferation.

Adhesion were measured using a wound healing assay. The assay showed a reduced rate of healing by 10.8% in cells with deficient LAMA5 compared to control cells ($92.8 \pm 1.6\%$ vs. $82.8 \pm 2.2\%$; $p = 0.0013$), indicating diminished adhesion properties (Fig. 6g). No changes in cell survival or proliferation were detected (Fig. 6h). These results confirmed a disruption in cellular focal adhesion properties in LAMA5 defective cells by altered cytoskeletal architecture, vinculin localization, and diminished cell healing.

2.6. Defective LAMA5 alters WNT signaling

Based on the radiographic phenotype that included decreased mineralization of the axial and appendicular bone, we investigated whether altered WNT signaling could contribute to the phenotype since loss of WNT signaling negatively impacts skeletal

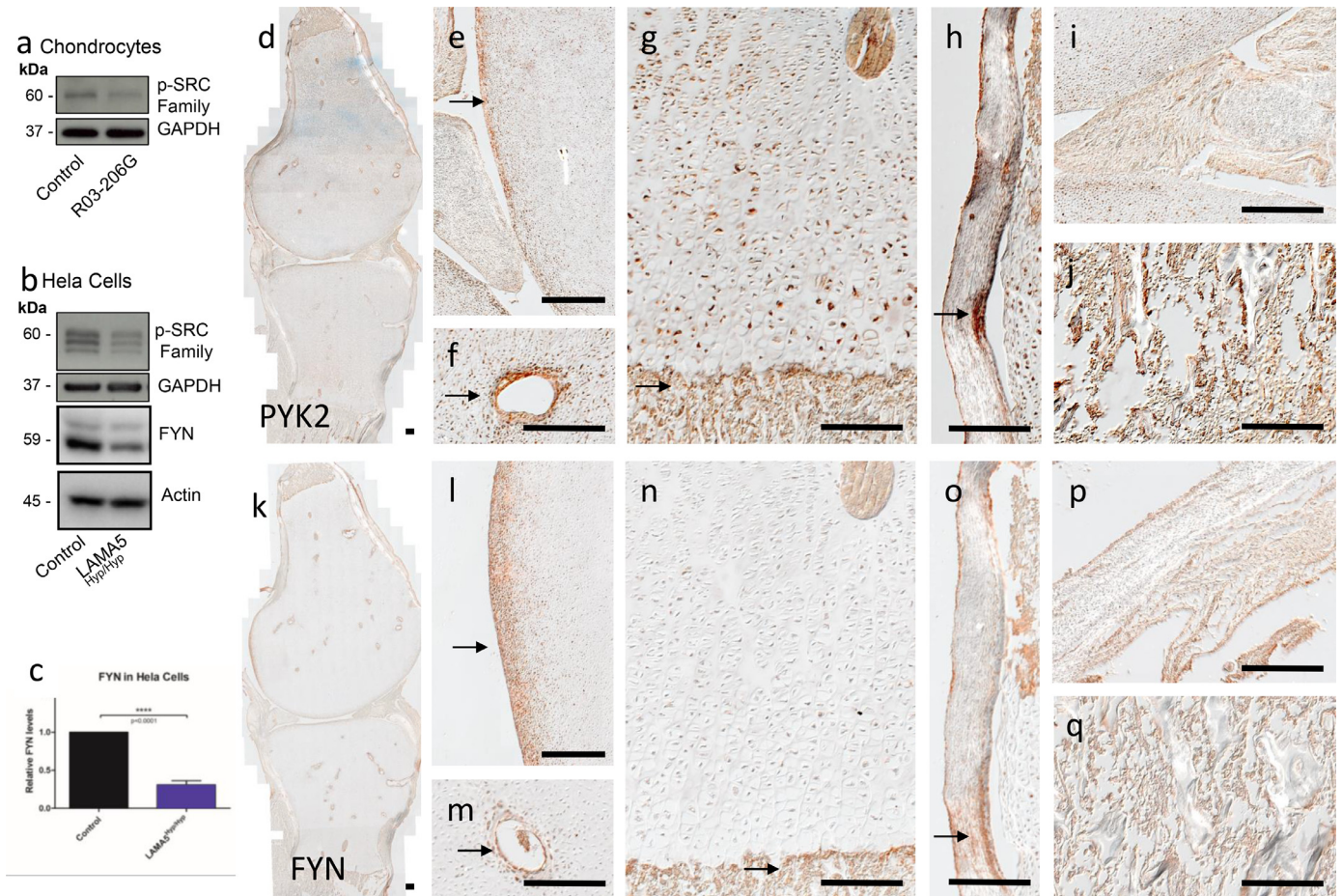


Fig. 5. LAMA5 mutant chondrocytes and LAMA5^{Hyp/Hyp} HeLa cells dysregulate SRC kinase expression levels. (a) Chondrocytes from R03–206 G showed decreased levels of p-SRC family. (b) A similar decrease in p-SRC family, as well as in FYN, was observed in HeLa LAMA5^{Hyp/Hyp} cells. (c) Quantitation of the decreased FYN levels in LAMA5^{Hyp/Hyp} HeLa cells shown in b. (d–j) PYK2 localizes similarly to LAMA5 around blood vessels in cartilage, ligaments and bone as well as articular cartilage growth plate and periosteum/perichondrium in human skeletal tissue. (k–q) FYN shows a very similar pattern with the exception of proliferative and hypertrophic growth plate chondrocytes, where it was not seen. Bars represent 50μm.

mineralization [30]. WNT signaling, both canonical and noncanonical, are active in many different cellular contexts to regulate development, growth, and maintenance. In canonical signaling, secreted WNT ligands bind to Frizzled receptors, leading to a larger receptor complex with co-receptors LRP5/6. This leads to the dissolution of a cytoplasmic β -catenin destruction complex consisting of DVL/APC/Axin/GSK3 β /CK1 α . Dissolution of the destruction complex allows for accumulation of cytoplasmic β -catenin, which then translocates to the nucleus to activate downstream targets (Figure S4). Src family kinases, including Src and FYN, have been implicated in canonical WNT signaling and have been shown to bind to LRP5/6, Frizzled and DVL2 in different contexts [31, 32] and FYN has been shown to directly stabilize β catenin in osteoarthritic cartilage [33].

To investigate WNT signaling we analyzed the TCF/LEF promoter activity after WNT3A induction. Both patient chondrocytes and LAMA5^{Hyp/Hyp} cells showed decreased TCF/LEF promoter activity (Fig. 7a–b). Analysis of the intracellular activation of WNT signaling after WNT3A treatment showed a reduction in phosphorylation of the WNT receptor LRP6 in patient chondrocytes at Ser 1490 (Fig. 7c–e). LAMA5^{Hyp/Hyp} cells also showed a reduction in LRP6 phosphorylation after WNT3A treatment, similar to patient chondrocytes (Fig. 7f–h). These results indicate that defective expression of LAMA5 diminished activation of the WNT pathway likely through decreased active Src and FYN kinases.

3. Discussion

We identified biallelic mutations in LAMA5 that resulted in decreased Laminin α 5 protein and produced a previously undescribed recessively inherited bent bone skeletal dysplasia. There have been two previous reports of LAMA5 variants in humans. In one report, heterozygosity for a LAMA5 mutation, c.9418G>A (p.V3140M), in one individual was associated with skin anomalies, muscle weakness, osteoarthritis, ligamentous laxity, and with other symptoms; however, although the variant altered a highly conserved residue, it was also found in unaffected individuals in the family [34]. In the other report, there was homozygosity for the LAMA5 variant c.8046C>T (p.Arg2659Trp) in an individual who presented with pre-synaptic myasthenic syndrome (hypotonia at birth, muscle weakness, respiratory failure requiring intermittent ventilation as a teen, ptosis, myopia, and facial tics). The authors showed that LAMA5 was expressed in nerve endplates and that the patient's endplates were morphologically abnormal [35]. The substituted arginine is not fully conserved across species, and the affected individual was also homozygous for a variant in LAMA1 (p.Asp210Asn) that altered a highly conserved residue and is predicted to be damaging. The asymptomatic parents were heterozygous for both of these variants [35]. These reports illustrate the potential for defective LAMA5 to produce disease, though the phenotypes differ from each other and our findings.

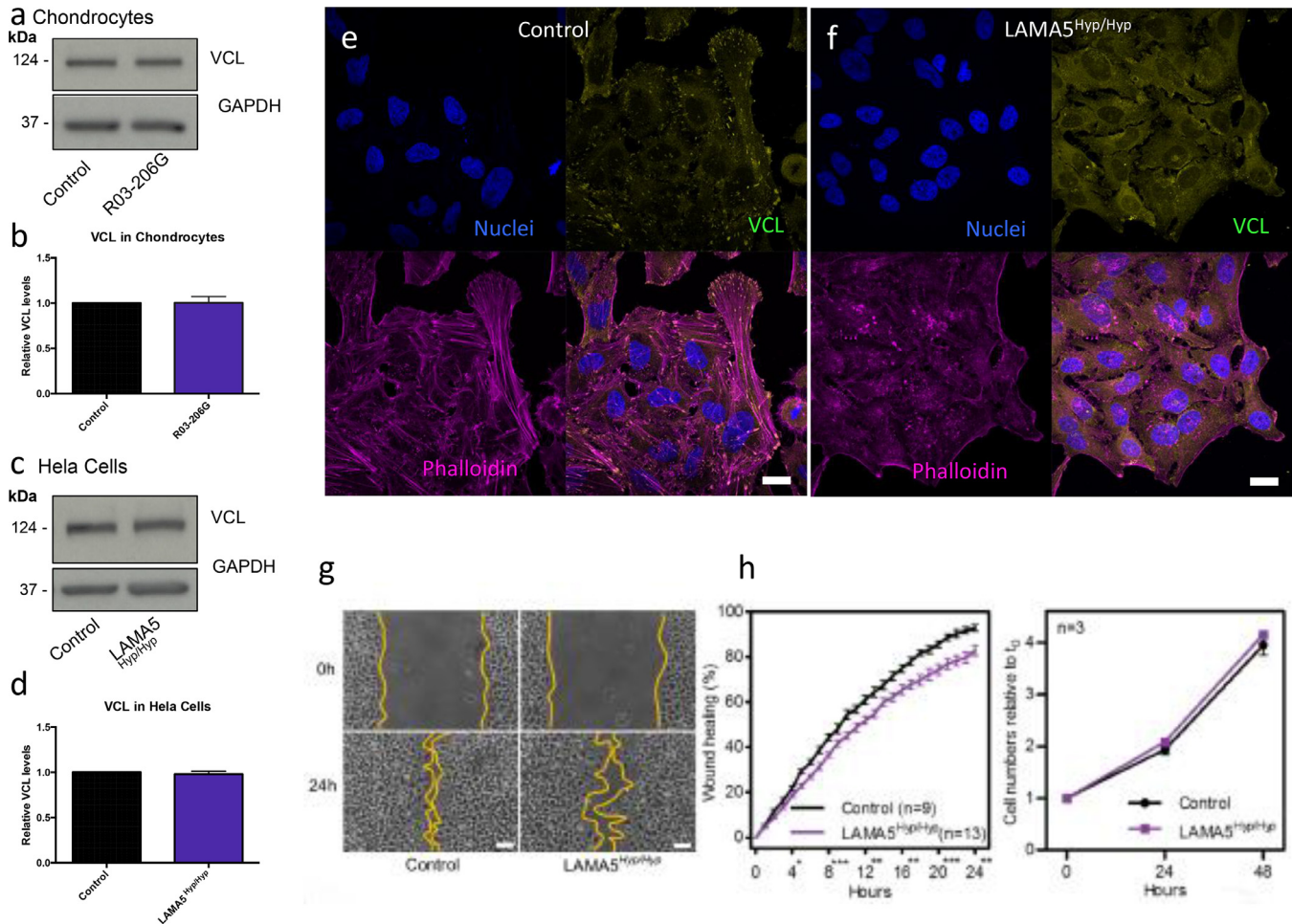


Fig. 6. Effects on cell adhesion due to loss of LAMA5

(a) Chondrocytes from R03–206 G and (c) LAMA5^{Hyp/Hyp} HeLa cells showed no change in total VCL levels compared to controls. (b,d) Quantitation of the data shown in a, b. (e-f) Focal adhesions were visualized by immunostaining with anti-VCL (green) and actin marker phalloidin (red). Nuclei were stained with DAPI (blue). Bars represent 20 μ m. (g) LAMA5^{Hyp/Hyp} HeLa cells have deficient migration. The LAMA5^{Hyp/Hyp} cells healed more slowly than the control cells at 24 h ($92.8 \pm 1.6\%$ vs. $82.8 \pm 2.2\%$ ($p = 0.0013$)). The orange lines indicate borders of the cell-less regions. Scale bars, 100 μ m. (h) Equal numbers of HeLa cells were plated and the cell numbers were calculated on three consecutive days and plotted as values relative to the first day of measurement (t₀). No differences in proliferation between control and LAMA5^{Hyp/Hyp} cells were found.

The phenotype we identified was consistent among the three affected siblings and included defects in the both the axial and appendicular skeleton, with radiographic findings showing undermineralized bone and a distinct angulation of the mid femoral shaft (Fig. 1 and Table S1). The phenotype also included extraskeletal features. There were facial dysmorphisms, abnormally formed ears with tags, wide-spaced nipples, and atrial septal defects, among other findings (Table S1). This disorder also likely includes abnormalities in muscle function based on the presence of elbow fusions, ulnar flexion contractions at the wrist (arthrogryposis multiplex congenita), bilateral talipes equinovarus, and failure to mount a respiratory effort at birth. Immunohistochemistry generated in both human and mouse tissues showed that LAMA5 was expressed in muscle and it has been previously reported that LAMA5 deficient intestine displayed a smooth muscle defect [36]. Laminins, type IV collagen, agrin, nidogen, biglycan, and perlecan form the basal lamina that surrounds skeletal muscle fibers, and it has been suggested that laminin in the ECM stimulates myoblast proliferation and differentiation [37, 38]. Thus, the potential for abnormal muscular function due to loss of LAMA5 is of particular interest in this disorder since muscle defects have also been speculated to contribute to bending of appendicular bones by altered mechanical forces during development [38].

Skeletal growth, in both the prenatal and postnatal periods, requires a series of tightly coordinated processes of cell proliferation, differentiation, migration of cells, mineralization, and expansion of the local vasculature. Both chondrocytes and osteoblasts contribute to angiogenesis by release of vascular endothelial growth factor (VEGF), furthering vessel formation through activation of VEGF receptors in endothelial cells. Blood vessels provide nutrients, oxygen, growth factors and hormones, as well as attracting progenitor cells. Type H vessels are a specialized subtype of capillary that expresses high levels of CD31 and endomucin, and these vessels are located near the growth plate in the metaphysis, the periosteum, and the endosteum of the diaphysis. Type H vessels are densely surrounded by osteoprogenitors [39] and aid in modulating osteoblasts, coupling osteogenesis to angiogenesis. There is also an embryonically expressed vessel termed Type E, with a similar expression pattern to type H vessels, but in mice they are highly expressed at E16.5 and then exhibit diminished expression by P28 [19]. Both Type E and Type H vessel endothelial cells have enriched expression of LAMA4, LAMA5, and β 1 Integrin, as well as extracellular matrix proteins, basement membrane and cell adhesion components [19]. Our immunohistochemistry findings expand on the role of LAMA5 expression in musculoskeletal development beyond the

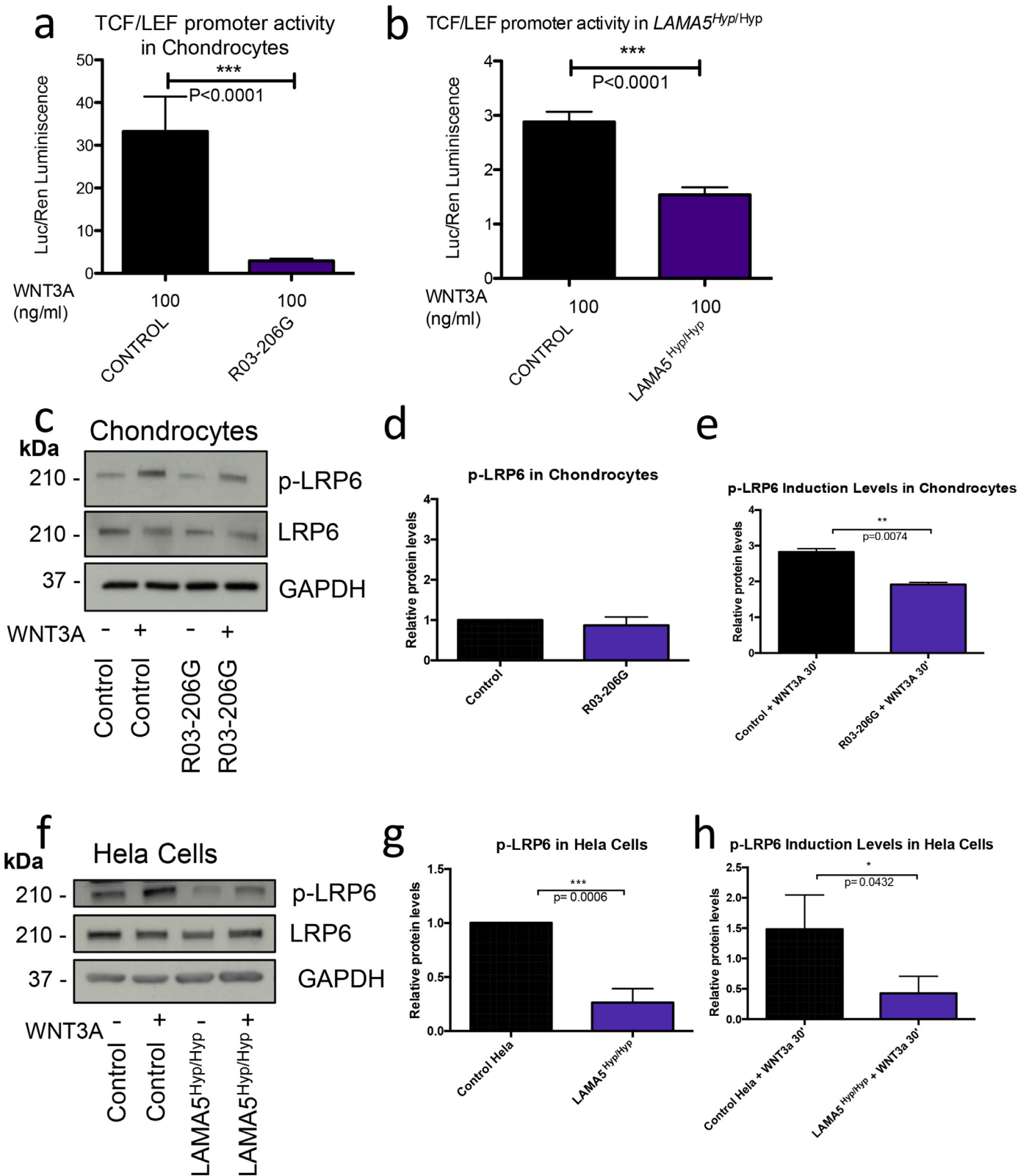


Fig. 7. Defective LAMA5 alters WNT signaling pathway. (a) TCF/LEF promoter showed a decreased activity in R03–206G patient chondrocytes when induced with 100 ng/ml WNT3A for 30 min. (b) Similar changes were observed in *LAMA5^{Hyp/Hyp}* cells after application of 100 ng/ml WNT3A. (c–h) Defective LAMA5 cells showed reduced LRP6 phosphorylation after a 30-minute incubation with 50 ng/ml WNT3A. * $p < 0.05$, ** $p < 0.01$, **** $p < 0.0001$.

previously described Type E capillaries, with expression in blood vessels in cartilage and ligament and expression in muscle, ligaments, periosteum, trabecular bone and throughout the cartilage, particularly in the growth plate and articular chondrocytes.

The functionality of laminins in general, including LAMA5, is mediated through interactions with cell membrane receptors; the most established LAMA5-receptor interaction is with $\beta 1$ Integrin. This study uncovered that the LAMA5- $\beta 1$ Integrin interaction was

altered by mutation and employed a non-canonical focal adhesion signaling pathway and the results are summarized in Table 2. Focal adhesion signaling typically transduces integrin intracellular signals through phosphorylation of FAK [40, 41]. This was not the case for signaling initiated by LAMA5, which induced the phosphorylation of PYK2. PYK2 belongs to the same family as FAK and has similar functions in cell migration, differentiation, and survival [42]. PYK2 has been described as an important factor in osteogenesis with roles in promoting osteoblast differentiation [27, 43–46], regulating osteoclastogenesis and bone remodeling [47–50] and modulating chondrogenesis [51–53]. Our study provides novel data that LAMA5 is required for PYK2 activation in the skeleton. Our results further show that the most relevant SRC family member downstream of PYK2 is FYN showing a similar skeletal localization to LAMA5. The importance of FYN in the skeleton is also supported by several studies that implicate FYN in osteoblast differentiation [54, 55], osteoclastogenesis [56, 57], and in cartilage differentiation/proliferation [58] and osteoarthritis, which is associated with an upregulation of FYN [33].

This skeletal specific signaling of PYK2 and FYN also suggests interactions of these kinases with important differentiation signaling pathways. Although PYK2 and FAK are very similar, they exhibit different effects on cellular behavior, likely dependent on tissue type. FAK activation causes cell spreading and pro-survival, while PYK2 induces reorganization of the cytoskeleton, cell detachment, and apoptosis [59]. PYK2 is known to stimulate multiple oncogenic signaling pathways including WNT [60, 61]. High levels of PYK2 levels are associated with poor cancer prognosis, in part through activation of WNT signaling [60]. Our findings show that diminished WNT3A-stimulated WNT signaling was seen in LAMA5 deficient cells through decreased LRP6 receptor levels with decreased responsiveness of the TCF/LEF reporter, a readout for β -catenin activity. Loss of the LAMA5 diminished PYK2 and FYN kinase activity and likely negatively impacted canonical WNT signaling as shown by decreased activation of β -catenin. This is in contrast to the work done by Rite et al., that showed that Lama5 may be a negative regulator of WNT signaling, particularly in intestinal cells [62]. However, it is possible that LAMA5 has cell context specific effects on WNT signaling.

The identification of this previously uncharacterized bent bone dysplasia offered a unique opportunity to understand the effects of LAMA5 and focal adhesion components in the skeleton, especially since the knock-out mouse models for *Lama5* are lethal [3]. Defective LAMA5 in LAMA5^{Hyp/Hyp} cells negatively impacted the organization of the actin cytoskeleton, vinculin localization, an important stabilizer of the focal adhesion complex, and cell migration, illustrating that, in part, the phenotype likely results from altered focal adhesions. The findings also support that, in the skeleton, a novel ECM network is induced through LAMA5- β 1 Integrin-PYK2-FYN (Figure S4) signaling, impacting WNT signaling, and underscoring the importance of basement membrane proteins in skeletogenesis beyond their structural support role to the cell.

4. Materials and methods

4.1. Ethics

This study was approved by the University of California at Los Angeles Institutional Review Board under protocol number IRB#14-00017. Informed consent was obtained from all participants.

4.2. Study design

Patients and their unaffected family members were ascertained under an IRB-approved human subject's protocol. Clinical information and imaging were obtained from review of all available medical records. All experiments performed in cells were conducted at least

three independent times and all replicates were included in our data analyses.

4.3. Cell culture

Dermal fibroblast cultures were established from explanted skin biopsies from one of the individuals with mutations in LAMA5 (International Skeletal Dysplasia Registry reference number R03–206G) and three controls. Primary chondrocytes were isolated from distal femurs of the same affected individual (R03–206G) and six age-matched normal controls by incubation of fragmented cartilage with 0.03% bacterial collagenase II. LAMA5^{Hyp/Hyp} HeLa cells generated by CRISPR/Cas9 and controls were purchased from Canopy Biosciences (catalog no. KOCE011980). All cells were grown in Dulbecco-Vogt Modified Eagle Medium (DMEM) supplemented with 10% fetal bovine serum (FBS).

All cells were grown to 100% confluence for at least 24 h. Stimulation experiments were conducted in DMEM with 10% FBS with either TGF β -1 (catalog no. 240-B, R&D Biosystems, 5 ng/ml with Ascorbic Acid, 50 ng/ml) or WNT3A (catalog no. 5036-WN, R&D Biosystems, 100 ng/ml). For protein analyses, cells were collected in IP Lysis Buffer (Thermo Scientific, 87,787) supplemented with proteinase inhibitors.

4.4. Exome analysis

DNA was isolated and submitted to the University of Washington Center for Mendelian Genomics for library preparation and exome sequencing. The samples were barcoded, captured using the Nimble-Gen SeqCap EZ Exome Library v2.0 probe library targeting 36.5 Mb of genome, and sequenced on the Illumina GAIIX platform with 50 bp bidirectional reads. Novoalign was used to align the sequencing data to the human reference genome (NCBI build 37) and the Genome Analysis Toolkit (GATK) was used for post-processing and variant calling according to GATK Best Practices recommendations. For each sample, at least 90% of targeted bases were covered by at least 10 independent reads. Variants were filtered against NIEHS EGP exome samples (v.0.0.8), exomes from the NHLBI Exome Sequencing Project (ESP6500), 1000 genomes (release 3.20120430), and in-house exome samples. Mutations were further compared with known disease-causing mutations in HGMD (2012.2). Variants were annotated using VAX, and mutation pathogenicity was predicted using the programs Polyphen, Sift, Condel, CADD, and MutationTaster (<http://www.mutationtaster.org/>). Potential disease-associated variants were identified under an autosomal recessive model, identifying either homozygosity for variants in one gene or compound heterozygosity for two variants in the same gene. The mutations reported in this work were confirmed by bidirectional Sanger sequencing of amplified DNA from the proband, siblings and the parents. Sequence trace files were aligned and analyzed using 4peaks.

4.5. Western blot

For Western blot analyses, protein lysates were separated by electrophoresis on 5%, 10%, or gradient (4 to 20%, catalog no. 4,568,093, Bio-Rad) SDS-polyacrylamide gels, transferred to polyvinylidene difluoride membranes, blocked in 5% milk, and probed overnight with primary antibody [anti-LAMA5 antibody (1:500; catalog no. C352437, LifeSpan Biosciences, Inc.), anti-Integrin β 1 (1:500; catalog no. AB1952, Chemicon), anti-phospho-FAK (1:1000; catalog no. 8556, Cell Signaling Technology), anti-phospho-Pyk2 (1:1000; catalog no. 3291, Cell Signaling Technology), anti-Pyk2 (1:1000; catalog no. 3292, Cell Signaling Technology), anti-phospho-Src Family (1:1000; catalog no. 6943, Cell Signaling Technology), anti-phospho-p130 Cas (1:1000; catalog no. 4011, Cell Signaling Technology), anti-p130 Cas (1:1000; catalog no. 610,271, BD Biosciences), anti-Vinculin (1:10,000; catalog no. 129,002, Abcam), anti-phospho-Paxillin

(1:1000; catalog no. 2541, Cell Signaling Technology), anti-phospho-LRP6 (1:1000; catalog no. 2568, Cell Signaling Technology), anti-LRP6 (1:1000; catalog no. 3395, Cell Signaling Technology), anti-FYN (1:1000; catalog no. 4023, Cell Signaling Technology), anti-GAPDH (1:2000; catalog no. 2118, Cell Signaling Technology), anti- β -Actin (1:1000; catalog no. 4967, Cell Signaling Technology), or anti- β -Tubulin (1:1000; catalog no. 2128, Cell Signaling Technology).

Peroxidase-conjugated secondary antibodies (1:2000, catalog nos. 7071 and 7072, Cell Signaling Technology) were used, and immunocomplexes were identified using the ECL (enhanced chemiluminescence) Detection Reagent (catalog no. 7003, Cell Signaling Technology). Fiji was used to quantify bands after gel analysis recommendations from ImageJ and Gassmann et al. (<http://rsb.info.nih.gov/ij/docs/menus/analyze.html#gels>), and the Student's *t*-test was performed for statistical analysis using Prism software. Experiments were replicated at least three times to perform statistical analysis.

4.6. Histological analyses and immunolocalization

For histology and immunocytochemistry, human (control) and mouse tissues (E18.5) were decalcified using immunocal decalcification solution (catalog no. 1414–1, StatLab), and then paraffin-embedded. Paraffin blocks were sectioned at 10 μ m.

For immunohistochemistry, paraffin sections were heated to 48 °C for 60 min in 0.2 M Sodium Citrate Buffer (pH 3.5). Primary antibodies used were: anti-LAMA5 (1:100; catalog no. C352437, LifeSpan Biosciences, Inc), anti-CD34 (1:100; catalog no. HPA036722, Prestige Antibodies), anti-p130[Cas] (1:100; catalog no. 610,271, BD Biosciences), anti-PYK2 (1:100; catalog no. 17,592–1-AP, Proteintech) and anti-FYN (1:2000; catalog no. 66,606–1-Ig, Proteintech). Sections were then incubated for 30 min in either R.T.U Biotinylated Goat Anti-Mouse IgG Antibody or R.T.U Biotinylated Goat Anti-Rabbit IgG Antibody (Vector Laboratories, catalog nos. BP-9100 and BP-9200). After a subsequent 30-minute incubation in Streptavidin Horseradish Peroxidase R.T.U. (Vector Laboratories, catalog no. 5704), the sections were stained using the ImmPACT DAB Peroxidase Substrate Kit (Vector Laboratories, catalog no. SK-4105).

Immunofluorescence experiments were performed using a Carl Zeiss LSM 700 laser scanning confocal microscope. Cultured cells were fixed in 4% PFA in PBS, then washed and permeabilized with 0.1% Triton X100 for 5 min, followed by blocking in 10% goat serum for 1 hour. The primary antibody was incubated overnight at 4 °C. Fluorescent secondary antibody was incubated at a 1:1000 dilution for 1 hour at room temperature (alexa-fluor goat anti-mouse 488 and goat anti-rabbit 568 for all samples), and DAPI at a 1:1000 dilution for 5 min at room temperature was applied before mounting.

For focal adhesion imaging, Hela cells were plated on glass coverslips, grown overnight and fixed using 4% paraformaldehyde for 15 min. Polymerized F-actin was visualized using Alexa Fluor 594–conjugated Phalloidin (Life Technologies), and vinculin was stained with vinculin–fluorescein isothiocyanate antibody (Sigma-Aldrich) according to the manufacturer's protocols.

4.7. Cartilage studies

Cartilage studies for protein levels were performed using lysates from frozen distal femur cartilage from proband R03-206G. Briefly, frozen cartilage was pulverized in liquid nitrogen and lysates were preserved in Proteinase and Phosphate inhibitors (Thermo Scientific 78440). Western blots were performed as described above.

4.8. Luciferase reporter assay

The TCF/LEF promoter reporter was purchased from Lenti-Signal, Qiagen. The Renilla control was used to normalize the luciferase signal (Lenti SIGNAL, Qiagen). Cells were transduced at 80% confluence.

When cells reached confluence, they were treated with 100 ng/ml WNT3A, (RnD System) and incubated overnight. Then, cells were lysed and luciferase activity was determined using a Dual-Luciferase Reporter Assay (Promega).

4.9. RNA extraction and qPCR

RNA was extracted from primary chondrocytes and Hela cells using TRIzol reagent (catalog no. 15-596-018, Life Technologies). Complementary DNA (cDNA) was prepared from 1 μ g of RNA using RevertAid First strand cDNA synthesis kit (Thermo Fisher Scientific) and amplified using Maxima SYBR Green/ROX qPCR Master Mix (catalog no. 11762100, Thermo Fisher Scientific). Gene expression was calculated using the $2^{-\Delta\Delta CT}$ method of analysis against the stable housekeeping gene β -2-microglobulin (β 2M). Three experimental replicates were performed with three technical replicates. qPCR primers were: β 2M: Fw: TGACTTTGTCACAGCCCAAG and Rev: AGCAAG-CAAGCAGAATTTGG. LAMA5: Fw: CGAGGACCTTACTGCAAGC and Rev: GGTGACGTTGACCTCGTTGT.

4.10. Migration and wound healing assays

For the wound healing assay, 250,000 Hela cells were plated in each well of 24-well plates. The next day, a single wound was introduced to each well using a 20 μ l filter tip scratch; the wells were then washed with PBS to remove detached cells and given 1 ml of fresh medium. The wounds were monitored in an automated incubation microscope BioStation CT (Nikon) in 1-hour intervals for 24 h. Wound widths were measured in ImageJ (<https://imagej.nih.gov/ij/>) using three measurements per image that were averaged to obtain a single value for each time point. Only wounds with initial widths of 700–900 μ m were included in each analysis.

For the cell tracking migration assay, 4000 Hela cells were plated in 24-well plates. Starting the next day, the cells were monitored in an automated incubation microscope BioStation CT in 5–10-minute intervals for 24 h. The trajectories were manually tracked using the ImageJ Manual Tracking plugin (<https://imagej.nih.gov/ij/plugins/track/track.html>), with the beginning and end of the measurement represented by two cell divisions. The length of the cell trajectories and the spatial (euclidean) distance between their beginnings and ends were analyzed using the Chemotaxis and Migration Tool 2.0 (ibidi).

4.11. Statistical analysis

GraphPad Prism was used for statistical analysis. All values are means \pm SEM, as indicated in the Figure Legends. All comparisons in the study were performed using the Student's *t*-test.

Funding

D.K. and D.H.C. are supported by the NIH grants [R01 AR066124](#), [R01 DE019567](#), [R01 HD070394](#). Sequencing was provided by the University of Washington Center for Mendelian Genomics (UWCMG) which is funded by the National Human Genome Research Institute (NHGRI) and the National Heart, Lung and Blood Institute (NHLBI) Award [1U54HG006493](#). P.K. was supported by the Ministry of Education, Youth and Sports of the Czech Republic (Grant [INTER-ACTION LTAUSA19030](#)); the Agency for Healthcare Research of the Czech Republic (Grant [NV18-08-00567](#)); and the Czech Science Foundation (Grant [GA19-20123S](#)).

Contributions

M.B., F.C., M.K.B., J.H.M., J.Z., I.D. performed the molecular experiments. W.Z., S.P.T., J.X.C., M.B., D.N. performed and were responsible

for the genomic analyses. D.H.C., R.S.L., and D.K. performed the clinical and radiographic assessment. D.H.C., P.K., I.D., and D.K. conceived the study design. M.B., I.D., D.H.C., P.K., and D.K. wrote the paper. The authors read and approved the final version of the manuscript.

Role of funding source

The funding sources which include NIH awards R01 AR066124, R01 DE019567, R01 HD070394, and U54HG006493, and Czech Republic grants INTER-ACTION LTAUSA19030, V18-08-00567 and GA19-20123S did not have any role in study design, data collection, data analyses, interpretation or writing of report.

Declaration of Competing Interest

The authors have no financial or personal interests to disclose.

Acknowledgments

We thank the family for their participation in this study.

Supplementary materials

Supplementary material associated with this article can be found, in the online version, at doi:10.1016/j.ebiom.2020.103075.

References

- Frantz C, Stewart KM, Weaver VM. The extracellular matrix at a glance. *J Cell Sci* 2010;123(Pt 24):4195–200.
- Miner JH. Developmental biology of glomerular basement membrane components. *Curr Opin Nephrol Hypertens* 1998;7(1):13–9.
- Miner JH, Cunningham J, Sanes JR. Roles for laminin in embryogenesis: exencephaly, syndactyly, and placental pathology in mice lacking the laminin alpha5 chain. *J Cell Biol* 1998;143(6):1713–23.
- Yao Y. Laminin: loss-of-function studies. *Cell Mol Life Sci* 2017;74(6):1095–115.
- Aumailley M, Bruckner-Tuderman L, Carter WG, Deutzmann R, Edgar D, Ekblom P, et al. A simplified laminin nomenclature. *Matrix Biol* 2005;24(5):326–32.
- Clause KC, Barker TH. Extracellular matrix signaling in morphogenesis and repair. *Curr Opin Biotechnol* 2013;24(5):830–3.
- Makrilia N, Kollias A, Manolopoulos L, Syrigos K. Cell adhesion molecules: role and clinical significance in cancer. *Cancer Invest* 2009;27(10):1023–37.
- Cary LA, Han DC, Polte TR, Hanks SK, Guan JL. Identification of p130Cas as a mediator of focal adhesion kinase-promoted cell migration. *J Cell Biol* 1998;140(1):211–21.
- Calderwood DA, Ginsberg MH. Talin forges the links between integrins and actin. *Nat Cell Biol* 2003;5(8):694–7.
- Danen EH, Yamada KM. Fibronectin, integrins, and growth control. *J Cell Physiol* 2001;189(1):1–13.
- Dayel MJ, Mullins RD. Activation of Arp2/3 complex: addition of the first subunit of the new filament by a WASP protein triggers rapid ATP hydrolysis on Arp2. *PLoS Biol* 2004;2(4):E91.
- Weed SA, Karginov AV, Schafer DA, Weaver AM, Kinley AW, Cooper JA, et al. Cortactin localization to sites of actin assembly in lamellipodia requires interactions with F-actin and the Arp2/3 complex. *J Cell Biol* 2000;151(1):29–40.
- Mortier GR, Cohn DH, Cormier-Daire V, Hall C, Krakow D, Mundlos S, et al. Nosology and classification of genetic skeletal disorders: 2019 revision. *Am J Med Genet A* 2019;179(12):2393–419.
- Wagner T, Wirth J, Meyer J, Zabel B, Held M, Zimmer J, et al. Autosomal sex reversal and campomelic dysplasia are caused by mutations in and around the SRY-related gene SOX9. *Cell* 1994;79(6):1111–20.
- Lim J, Grafe I, Alexander S, Lee B. Genetic causes and mechanisms of osteogenesis imperfecta. *Bone* 2017;102:40–9.
- Merrill AE, Sarukhanov A, Krejci P, Idoni B, Camacho N, Estrada KD, et al. Bent bone dysplasia-FGFR2 type, a distinct skeletal disorder, has deficient canonical FGF signaling. *Am J Hum Genet* 2012;90(3):550–7.
- Huber C, Cormier-Daire V. Ciliary disorder of the skeleton. *Am J Med Genet C Semin Med Genet* 2012;160C(3):165–74.
- Cormier-Daire V, Genevieve D, Munnich A, Le Merrer M. New insights in congenital bowing of the femora. *Clin Genet* 2004;66(3):169–76.
- Langen UH, Pitulescu ME, Kim JM, Enriquez-Gasca R, Sivaraj KK, Kusumbe AP, et al. Cell-matrix signals specify bone endothelial cells during developmental osteogenesis. *Nat Cell Biol* 2017;19(3):189–201.
- Li S, Qi Y, McKee K, Liu J, Hsu J, Yurchenco PD. Integrin and dystroglycan compensate each other to mediate laminin-dependent basement membrane assembly and epiblast polarization. *Matrix Biol* 2017;57–58:272–84.
- Ayturk UM, Jacobsen CM, Christodoulou DC, Gorham J, Seidman JG, Seidman CE, et al. An RNA-seq protocol to identify mRNA expression changes in mouse diaphyseal bone: applications in mice with bone property altering *Lrp5* mutations. *J Bone Miner Res* 2013;28(10):2081–93.
- Tiwari S, Askari JA, Humphries MJ, Bulleid NJ. Divalent cations regulate the folding and activation status of integrins during their intracellular trafficking. *J Cell Sci* 2011;124(Pt 10):1672–80.
- Lopez-Ceballos P, Herrera-Reyes AD, Coombs D, Tanentzapf G. In vivo regulation of integrin turnover by outside-in activation. *J Cell Sci* 2016;129(15):2912–24.
- Toya SP, Wary KK, Mittal M, Li F, Toth PT, Park C, et al. Integrin alpha6beta1 Expressed in ESCs Instructs the Differentiation to Endothelial Cells. *Stem Cells* 2015;33(6):1719–29.
- Owen KA, Pixley FJ, Thomas KS, Vicente-Manzanares M, Ray BJ, Horwitz AF, et al. Regulation of lamellipodial persistence, adhesion turnover, and motility in macrophages by focal adhesion kinase. *J Cell Biol* 2007;179(6):1275–87.
- Loeser RF. Integrins and cell signaling in chondrocytes. *Biorheology* 2002;39(1–2):119–24.
- Eleniste PP, Patel V, Posritong S, Zero O, Largura H, Cheng YH, et al. Pyk2 and megakaryocytes regulate osteoblast differentiation and migration via distinct and overlapping mechanisms. *J Cell Biochem* 2016;117(6):1396–406.
- Li B, Balasubramanian K, Krakow D, Cohn DH. Genes uniquely expressed in human growth plate chondrocytes uncover a distinct regulatory network. *BMC Genomics* 2017;18(1):983.
- Roca-Cusachs P, del Rio A, Puklin-Faucher E, Gauthier NC, Biaias N, Sheetz MP. Integrin-dependent force transmission to the extracellular matrix by alpha-actinin triggers adhesion maturation. *Proc Natl Acad Sci U S A* 2013;110(15):E1361–70.
- Laine CM, Joeng KS, Campeau PM, Kiviranta R, Tarkkonen K, Grover M, et al. WNT1 mutations in early-onset osteoporosis and osteogenesis imperfecta. *N Engl J Med* 2013;368(19):1809–16.
- Villarreal A, Del Valle-Perez B, Fuertes G, Curto J, Ontiveros N, Garcia de Herreros A, et al. SRC and FYN define a new signaling cascade activated by canonical and non-canonical Wnt ligands and required for gene transcription and cell invasion. *Cell Mol Life Sci* 2020;77(5):919–35.
- Yokoyama N, Malbon CC. Dishevelled-2 docks and activates SRC in a WNT-dependent manner. *J Cell Sci* 2009;122(Pt 24):4439–51.
- Li K, Zhang Y, Zhang Y, Jiang W, Shen J, Xu S, et al. Tyrosine kinase Fyn promotes osteoarthritis by activating the beta-catenin pathway. *Ann Rheum Dis* 2018;77(6):935–43.
- Sampaolo S, Napolitano F, Tirozzi A, Reccia MG, Lombardi L, Farina O, et al. Identification of the first dominant mutation of LAMA5 gene causing a complex multi-system syndrome due to dysfunction of the extracellular matrix. *J Med Genet* 2017;54(10):710–20.
- Maselli RA, Arredondo J, Vazquez J, Chong JX, University of Washington Center for Mendelian G, Bamshad MJ, et al. Presynaptic congenital myasthenic syndrome with a homozygous sequence variant in LAMA5 combines myopia, facial tics, and failure of neuromuscular transmission. *Am J Med Genet A* 2017;173(8):2240–5.
- Bolcato-Bellemin AL, Lefebvre O, Arnold C, Sorokin L, Miner JH, Kedinger M, et al. Laminin alpha5 chain is required for intestinal smooth muscle development. *Dev Biol* 2003;260(2):376–90.
- Rooney JE, Gurpur PB, Burkin DJ. Laminin-111 protein therapy prevents muscle disease in the mdx mouse model for Duchenne muscular dystrophy. *Proc Natl Acad Sci U S A* 2009;106(19):7991–6.
- Sharif A, Stern T, Rot C, Shahar R, Zelzer E. Muscle force regulates bone shaping for optimal load-bearing capacity during embryogenesis. *Development* 2011;138(15):3247–59.
- Zhao Y, Xie L. Unique bone marrow blood vessels couple angiogenesis and osteogenesis in bone homeostasis and diseases. *Ann N Y Acad Sci* 2020.
- Petit V, Thiery JP. Focal adhesions: structure and dynamics. *Biol Cell* 2000;92(7):477–94.
- Sieg DJ, Hauck CR, Ilic D, Klingbeil CK, Schaefer E, Damsky CH, et al. FAK integrates growth-factor and integrin signals to promote cell migration. *Nat Cell Biol* 2000;2(5):249–56.
- Zhao J, Zheng C, Guan J. Pyk2 and FAK differentially regulate progression of the cell cycle. *J Cell Sci* 2000;113(Pt 17):3063–72.
- Li X, Ye JX, Xu MH, Zhao MD, Yuan FL. Evidence that activation of ASIC1a by acidosis increases osteoclast migration and adhesion by modulating integrin/Pyk2/Src signaling pathway. *Osteoporos Int* 2017;28(7):2221–31.
- Bonnette PC, Robinson BS, Silva JC, Stokes MP, Brosius AD, Baumann A, et al. Phosphoproteomic characterization of PYK2 signaling pathways involved in osteogenesis. *J Proteomics* 2010;73(7):1306–20.
- Posritong S, Hong JM, Eleniste PP, McIntyre PW, Wu JL, Himes ER, et al. Pyk2 deficiency potentiates osteoblast differentiation and mineralizing activity in response to estrogen or raloxifene. *Mol Cell Endocrinol* 2018;474:35–47.
- Buckbinder L, Crawford DT, Qi H, Ke HZ, Olson LM, Long KR, et al. Proline-rich tyrosine kinase 2 regulates osteoprogenitor cells and bone formation, and offers an anabolic treatment approach for osteoporosis. *Proc Natl Acad Sci U S A* 2007;104(25):10619–24.
- Xiong WC, Feng X, PYK2 and FAK in osteoclasts. *Front Biosci* 2003;8:d1219–26.
- Gil-Henn H, Destaing O, Sims NA, Aoki K, Alles N, Neff L, et al. Defective microtubule-dependent podosome organization in osteoclasts leads to increased bone density in *Pyk2(-/-)* mice. *J Cell Biol* 2007;178(6):1053–64.
- Lakkakorpi PT, Bett AJ, Lipfert L, Rodan GA, Duong LT. PYK2 autophosphorylation, but not kinase activity, is necessary for adhesion-induced association with c-Src, osteoclast spreading, and bone resorption. *J Biol Chem* 2003;278(13):11502–12.

- [50] Jin WJ, Kim B, Kim JW, Kim HH, Ha H, Lee ZH. Notch2 signaling promotes osteoclast resorption via activation of PYK2. *Cell Signal* 2016;28(5):357–65.
- [51] Arcucci A, Montagnani S, Gionti E. Expression and intracellular localization of Pyk2 in normal and v-src transformed chicken epiphyseal chondrocytes. *Biochimie* 2006;88(1):77–84.
- [52] Liang W, Li Z, Wang Z, Zhou J, Song H, Xu S, et al. Periodic mechanical stress induces chondrocyte proliferation and matrix synthesis via CaMKII-mediated Pyk2 signaling. *Cell Physiol Biochem* 2017;42(1):383–96.
- [53] Loeser RF, Forsyth CB, Samarel AM, Im HJ. Fibronectin fragment activation of proline-rich tyrosine kinase PYK2 mediates integrin signals regulating collagenase-3 expression by human chondrocytes through a protein kinase C-dependent pathway. *J Biol Chem* 2003;278(27):24577–85.
- [54] Lee YC, Huang CF, Murshed M, Chu K, Araujo JC, Ye X, et al. Src family kinase/abl inhibitor dasatinib suppresses proliferation and enhances differentiation of osteoblasts. *Oncogene* 2010;29(22):3196–207.
- [55] Kaabeche K, Lemonnier J, Le Mee S, Caverzasio J, Marie PJ. Cbl-mediated degradation of Lyn and Fyn induced by constitutive fibroblast growth factor receptor-2 activation supports osteoblast differentiation. *J Biol Chem* 2004;279(35):36259–67.
- [56] Kim HJ, Warren JT, Kim SY, Chappel JC, DeSelm CJ, Ross FP, et al. Fyn promotes proliferation, differentiation, survival and function of osteoclast lineage cells. *J Cell Biochem* 2010;111(5):1107–13.
- [57] Kim HS, Kim DK, Kim AR, Mun SH, Lee SK, Kim JH, et al. Fyn positively regulates the activation of DAP12 and FcRgamma-mediated costimulatory signals by RANKL during osteoclastogenesis. *Cell Signal* 2012;24(6):1306–14.
- [58] van Oosterwijk JG, van Ruler MA, Briaire-de Bruijn IH, Herpers B, Gelderblom H, van de Water B, et al. Src kinases in chondrosarcoma chemoresistance and migration: dasatinib sensitises to doxorubicin in TP53 mutant cells. *Br J Cancer* 2013;109(5):1214–22.
- [59] Bellido T. Antagonistic interplay between mechanical forces and glucocorticoids in bone: a tale of kinases. *J Cell Biochem* 2010;111(1):1–6.
- [60] Zhu X, Bao Y, Guo Y, Yang W. Proline-Rich Protein Tyrosine Kinase 2 in Inflammation and Cancer. *Cancers (Basel)* 2018;10(5).
- [61] Despeaux M, Chicanne G, Rouer E, De Toni-Costes F, Bertrand J, Mansat-De Mas V, et al. Focal adhesion kinase splice variants maintain primitive acute myeloid leukemia cells through altered Wnt signaling. *Stem Cells* 2012;30(8):1597–610.
- [62] Ritte L, Spenle C, Lacroute J, Bolcato-Bellemin AL, Lefebvre O, Bole-Feysot C, et al. Abnormal Wnt and PI3Kinase signaling in the malformed intestine of lama5 deficient mice. *PLoS ONE* 2012;7(5):e37710.